https://doi.org/10.46813/2024-154-078

# SPATIAL DISTRIBUTION OF ELECTRIC FIELD IN A TWO STAGE HALL TYPE PLASMA SOURCE

*V.Yu. Bazhenov, A.M. Dobrovolskii, V.V. Tsiolko, V.M. Piun*
*Institute of Physics NAS of Ukraine, Kyiv, Ukraine*
*E-mail: tsiolko@iop.kiev.ua*

The two-stage plasma source of Hall type having common anode and two cathodes residing at locations with essentially different magnetic field configuration is experimentally studied. Considered are peculiarities of spatial distribution of floating potential measured by moved Langmuir probes. In particular, it was established that in the middle plane of the anode on the axis of the device, the value of the floating potential of the plasma is up to 95% of the anode voltage.

PACS: 52.65.-y,52.25.Xz,52.27.Aj

## INTRODUCTION

Hall type plasma sources due to their simple design and high reliability of plasma generation in a wide range of conditions are widely used in science and technology. Previously, we created the anode layer based source of a cylindrical plasma flow with enhanced efficiency of the discharge volume usage [1]. The peculiarity of the source is the ionization of the working gas in the anode layer on the periphery of the beam diameter, the accumulation of space charge in the main part of the volume of the beam formation and the formation of the beam itself by the space charge field. The proposed design used two cathodes in the form of several rods that were located inside the anode symmetrically relative to the middle plane of the anode.

The authors of the present work earlier studied the modified version of the previous device in which one half of the cathode system was replaced by a ring-shaped cathode located in a region with weak magnetic field, so that instead of being symmetrical the system becomes a two-stage one [2]. At that, the working gas was injected along the axis of the system rather than through the anode. Such design looked a promising one from viewpoint of enhanced ion thrust due to optimizing the distribution of energy supplied by the power source between the stages of the device. Realization of such approach requires thorough study of the discharge plasma peculiarities occurring inside the device.

This paper presents the results of experimental studies of spatial distributions of the plasma floating potential inside the two stages of the proposed asymmetric discharge system with common anode and two cathodes residing at locations with essentially different magnetic field configuration.

## 1. EXPERIMENTAL DEVICE AND DIAGNOSTICS

The investigated device (Fig. 1) was placed inside a metal cylindrical vacuum chamber with a diameter of 500 mm, a length of 700 mm and a volume of 140 l on dielectric brackets. Also, a computer-controlled table for moving diagnostic tools along the axis of the camera with a minimum movement step of 1 mm was placed in the chamber.

Anode 3 of the device with an internal diameter of 59 mm and a length of 63 mm was located inside a quartz cylinder 4 with an internal diameter of 95 mm and a length of 150 mm.

The "internal" cathode C1 consisted of 6 rods with a diameter of 3 mm and a length of 20 mm located in a circle at a certain distance from the inner surface of the anode. The role of the "external" cathode C2 was performed by a metal ring with an inner diameter of 65 mm and a height of 20 mm. Cathode C2 was mounted on the output flange 7 with a thickness of 10 mm flush with the inner plane of the flange. The distance from the anode to the inner plane of the output flange 7 was 45 mm.

When conducting experimental studies, the pulse-periodic mode of operation of the power source was used in order to prevent overheating of the elements of both the source itself and the discharge system. At that, the anode voltage looked as an each two seconds repeated sequence of four half-sine shaped pulses with 50 Hz power net frequency. The maximum amplitude of the impulse voltage at the anode $U_a$ was 4.2 kV, and the maximum current through the cathodes C1, C2 was up to 0.5 A.

When measuring the floating potential, two slightly different L-shaped Langmuir probes were used, both with the same lengths of the receiving part of 5 mm made of tungsten with a diameter of 0.19 mm. Probe 1 with a ceramic holder diameter of 3.2 mm and a length of 220 mm was used to measure the floating potential both inside and outside the anode. This probe could move in the radial direction in the range of R = ±24 mm and in the longitudinal direction L = 0…165 mm (the size of L was measured from the end of the anode closest to the cathode C1). Probe 2 with a diameter of a glass holder of 5 mm was used to measure $U_f$ in the gap between the anode and the cathode C2 with a change in R within ± 48 mm.

When studying the properties of the device, measurements were made of voltages and currents of cathodes C1, C2 ($U_{c1}$, $U_{c2}$, $I_{c1}$, $I_{c2}$, respectively), the anode voltage $U_a$, the potential of the floating probe $U_f$ at an argon pressure in the chamber of $2.9 \cdot 10^{-4}$ Torr and values of the resistors R1=10 kΩ, R2=820 Ω.

A schematic representation of the shape of force lines of the magnetic field H of the device is shown in

Fig. 1 (the structure of the magnetic field is presented in more detail in [3]). The cusp planes with the zero value of the magnetic field were located at a distance of (23±1.5) mm from the anode ends.

Plasma emission spectra were studied using a CCD spectrometer SL40-2-2048 in the wavelength range of 400…900 nm with a resolution of about 0.5 nm. The radiation entered the spectrometer through an optical waveguide with an effective input diameter of about 0.4 mm. The projection of the radiation reception zone onto the entrance of the waveguide was carried out using a lens with a focal length of 105 mm and a relative aperture that could vary from 1:4.5 to 1:16.

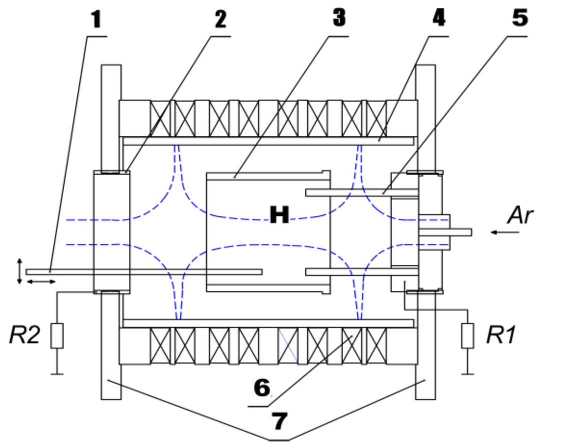


*Fig. 1. Scheme of experiment device:*
*1 – Langmuir probes; 2 – cathode 2 C2; 3 – anode;*
*4 – quartz cylinder; 5 – cathode 1 C1;*
*6 – magnet system; 7 – dielectric flanges with a thickness of 10 mm; H – magnetic field lines*

Note that even with the maximum aperture, the effective value was limited to about 1:8 due to the angular aperture of the waveguide. Such configuration was used in most studies, and only with very strong signals the relative aperture was reduced to 1:16. The length of the optical path from the lens to the center of the discharge system at the average position of the mirror was about 600 mm, which provided an effective diameter of the perception zone of about 2 mm with its effective length of about 100 mm for the correct measurement of transverse distributions inside the discharge area. The exposure time when recording the spectra was 0.1 s with a period of 2 s according to the discharge power mode. The duration of the recording cycle of the spatial distribution was 20 min, and the resulting array of 600 spectra was stored in a file using the spectrometer software for further processing.

## 2. EXPERIMENTAL RESULTS

Typical graphs of the anode voltage $U_a$ and the potential of the floating probe $U_f$ obtained when using probe 1 are presented in Fig. 2. Spikes of $U_a$, which are observed at duration of t up to ≈ 0.5 ms, are associated with transient processes that occur during the ignition of the discharge in the first stage between the anode and cathode C1. One can see that these fluctuations of the anode voltage with amplitude of up to 0.5…0.6 kV practically do not affect the value of $U_f$. After t ≈ 0.5 ms, the discharges in both stages operate in quasi-stationary modes, and about 80% of the energy is supplied to the discharge of the second stage of the device between the anode and the cathode C2. At durations t ≈ 4…8 ms $U_f$ changes synchronously with $U_a$ reaching maximum values at t ≈ 6 ms. At the same time, the potential difference $U_f$ - $U_a$ remains slightly variable. In subsequent, the maximum values of potentials and currents at t = 6 ms will be considered.

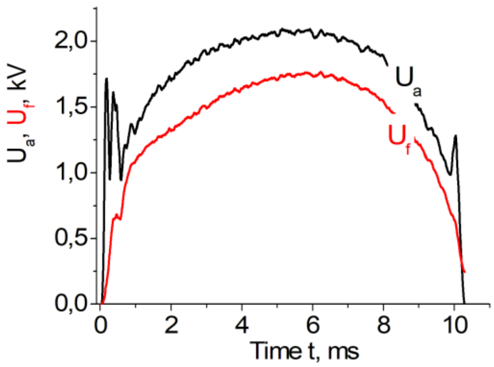


*Fig. 2. Typical graphs of the anode voltage $U_a$ and the potential of the floating probe $U_f$. at a distance of L=75 mm and R=20 mm*

Let's consider the results of measuring $U_f$ using probe 1. During the measurements, it turned out that placing the probe inside the anode at distances L ≈ 0…30 mm significantly affects the operating modes of the device. First of all, this leads to the dependence of the anode voltage $U_a$ on the position of the probe inside the anode cavity. In addition, moving the probe to radii R greater than ≈ 16 mm led to quenching the discharges in both stages of the device. At distances L greater than ≈ 30 mm, the influence of the location of the probe along L and R on the value of the anode voltage $U_a$ is significantly reduced. Therefore, the measurement results for this range of $U_a$ changes will be presented below.

Such a difference in the behavior of the anode voltage at distances L less than or greater than 30 mm is primarily related to the peculiarities of the types (and, accordingly, the character) of operating the discharges in the first and second stages of the device. If in the first stage we observe a variant of the discharge with an anode layer across the magnetic field, then in the second stage the discharge current is carried both across and along the magnetic field. In the second case, the effect of moving the probe holder on the discharge operation is reduced.

In the range of L values greater than 30 mm, the average value of $U_a$ was 2.050 kV. Moving the probe along L and R led to a change in the value of $U_a$ by only a few percent. Since the change in the value of $U_a$ is much smaller than the difference $U_f^{max} – U_a^{max}$, for the convenience of further comparing the results obtained at different L, R, we will give exactly the dependence of the values of $U_f^{max} – U_a^{max}$ on L, R. Fig. 3 shows the dependence of this potential difference on L at the system axis. The same figure shows the placement of particular electrodes in the discharge gaps and the position of the magnetic field cusp.

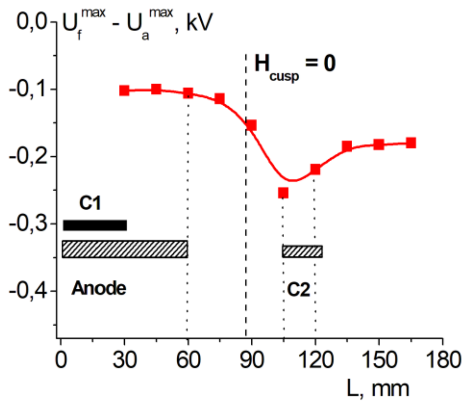


*Fig. 3. Dependence of maximum values* $U_f^{max} – U_a^{max}$ *on distance L at the system axis (R = 0)*

One can see from the figure that this dependence has a purely non-monotonic character. After leaving the anode cavity, the floating potential $U_f^{max}$ begins to drop sharply relatively to the anode voltage, increasing the potential difference from ≈ - 0.1 kV inside the anode to - 0.25 kV near the entrance to the cathode C2. With a further increase in L, the potential difference begins to decrease, reaching ≈ - 0.18 kV at L ≈ 145 mm.

The detailed radial distribution of $U_f^{max} – U_a^{max}$ at different distances L is presented in Fig. 4,a. If inside the anode (i.e. for L = 45, 60 mm) and outside the anode at distances L = 75, 90 mm, the radial distribution of the potential difference has a flat top within the range of changes in R values of approximately ± 16 mm and a sharp increase in this difference at larger R values, then at larger L the nature of the radial dependence significantly changes An increase in the distance L to 105 mm leads to a sharp increase in the potential difference on the axis of the system with a simultaneous decrease in this difference at larger radii R. A further increase in L to 135 mm leads to another change in the nature of the radial distribution of the potential difference $U_f^{max} – U_a^{max}$ – a decrease in the values on the axis and an increase at larger values of the radius R. That is, as in the case of the radial distribution at L = 45…90 mm, at distances L greater than ≈ 135 mm, the radial distribution becomes flatter. In general, in the range of changes of L ≈ 90…135 mm (that is, between the plane of the zero value of the magnetic field of the cusp and the exit from the ring cathode C2), a “dip” is observed in the axial region of the spatial distribution of the floating potential.

Fig. 4,b shows averaged over time and observation line radial dependences of intensities of the emission lines ArI, λ = 750.39 nm (transition $2p_1 \rightarrow 1s_2$, $E_{th}$ = 13.48 eV, σ = $512 \cdot 10^{-20}$ cm$^2$ at 25 eV, $418 \cdot 10^{-20}$ cm$^2$ at 50 eV), where $E_{th}$ – threshold excitation energy of level $2p_1$, σ – excitation cross-section.

At an argon pressure of < $10^{-3}$ Torr, the dominant mechanism in the occupation of the Ar ($2p_1$) level is excitation by an electron impact from the ground state, and the main part of the energy is emitted during the transition to the Ar($1s_2$) level [4].

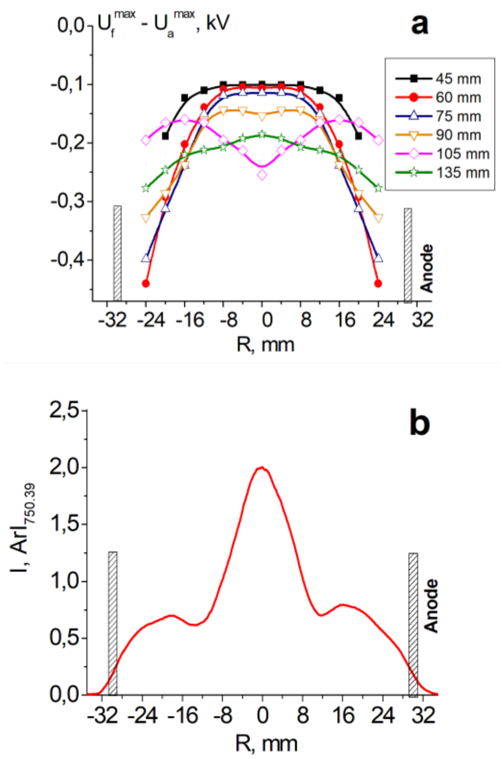


*Fig. 4. Radial dependencies of* $U_f^{max} – U_a^{max}$ *at different distances L (a); averaged over time and line of observation radial dependences of the emission line intensities for atomic argon ArI (750.39 nm) (b)*

The radiation intensity of the argon line is 750.39 nm $I_{750} \sim n_e f(\varepsilon)$ (ε> 14 eV), where $n_e$, f(ε) are the plasma density and the electron energy distribution function (EEDF), respectively. I.e. $I_{750}$ is a certain measure of the plasma density and the content of electrons with energy greater than ≈ 14 eV. In our case, it is assumed that f(ε) in the energy range ≈ (14…35) eV weakly depends on the R, L, so that radial density $I_{750}$ is similar to averaged over time and observation line radial dependence of the plasma density $n_e$. The radial dependence of $I_{750}$ has a bell-like shape within changes of R ≈ ± 12 mm, which at larger R turns into symmetrical “wings”. This form of radial density coincides with the results of visual monitoring of light emitted by the plasma in the device. The plasma emission in the device is a superposition of the bright light of the central plasma kernel and the less bright plasma of the tubular shape that embraces this kernel. This kernel with a diameter of ≈ 20…25 mm is placed in the middle of the anode cavity and ends at a distance of L ≈ 80…90 mm (that is, near the area of the zero value of the magnetic field of the cusp). It should also be added that the brightness of the plasma emission at higher values of L approximately corresponds to the brightness of light emitted by the plasma embracing the central kernel.

Comparison of Fig. 4,a,b shows that at L ≈ 45…90 mm a width of the “flat” part of radial dependence $U_f^{max} – U_a^{max}$ coincides with the zone of the most intense radiation of 750.39 nm line, and a sharp increase $U_f^{max} - U_a^{max}$ at radii larger than R ≈ 12 mm falls on the "wings" of the radiation intensity distribution $I_{750}$. All this gives reason to assume that the radial distribution of $I_{750}$ corresponds to the averaged distribution of the plasma density in the central plasma core at L < 90 mm.

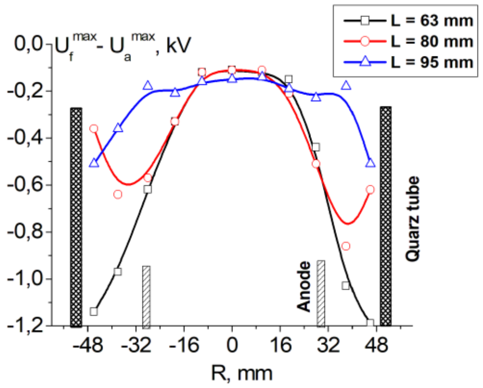


*Fig. 5. Radial dependencies of maximum values $U_f^{max} - U_a^{max}$ in the gap between the anode and the output flange with the cathode C2 at different distances from the anode L*

Fig. 5 exhibits the results of measuring $U_f$ using probe 2 inside the second stage of the discharge system, that is, in the space between the anode and the output plane. It should be noted that, unlike the case of the measurements in the first stage, placing the probe in any position practically does not affect the device operation. One can see that $U_f$ drops essentially deeper to the negative values at the periphery of plane located right after the anode end. Another peculiarity consists in non-monotonous variations of $U_f$ when the plane of measurements shifts towards the system output. The most flat radial dependence is observed in the plane corresponding to the magnetic field cusp. Such complex behavior is most probably due to the presence of dielectric wall which has ability to accumulate electric charge, namely, the electrons as it follows from the sign of the $U_f$ variations. The most efficient accumulation can occur in places where motion of the electrons towards the anode occurs across the magnetic field and is thus essentially more difficult. On the other side, in a space located closer to the magnetic field cusp the electrons can move freely and efficiently penetrate into the first stage of the device along the magnetic field lines. Thus, the second stage can serve as an efficient external electron source for the first stage of the device. Such suggestion can explain essentially uniform $U_f$ distribution inside the first stage and, most likely, is responsible for high efficiency of the device operation as a whole.

## SUMMARY

The experimental studies of spatial distributions of the plasma floating potential inside the two-stage discharge system have shown a number of essential peculiarities inherent to the system under study. In the first stage of the device with stronger magnetic field the radial distribution of the potential is practically uniform until about one half of the anode radius and is just about 100 V below the anode potential which varies from 1 to 2 kV. The second stage of the system, which is located closer to the magnetic field cusp, exhibits essentially non-monotonous spread of the potential. This stage likely serves an efficient source of electrons which are supplied to the first stage along the magnetic field lines and flatten radial potential distribution in there. Such behavior promotes higher efficiency of the plasma generation in the studied two-stage discharge system. After proper subsequent optimization of the geometry and electric power supply such system can become an efficient large aperture source of high energy ions.

## REFERENCES


1. I. Litovko, A. Goncharov, A. Dobrovolskyi, and I. Naiko. The Emerging Field Trends Erosion-Free Electric Hall Thrusters Systems // *Plasma Science and Technology* / Edited by Aamir Shahzad, InTechOpen, London, 2022. Chapter 11, p. 195-214. DOI: 10.5772/intechopen.99096.

2. V.Yu. Bazhenov, A.M. Dobrovolskiy, V.V. Tsiolko, V.M. Piun. Two stage plasma source for large scale beam generation // *Problems of Atomic Science and Technology. Series "Plasma Electronics and New Methods of Acceleration".* 2023, № 4, p. 121-124. DOI:10.46813/2023-146-121

3. A.M. Dobrovol's'kii, A.N. Evsyukov, A.A. Goncharov, I.M. Protsenko. Cylindrical magnetron based on the plasmaoptical principles // *Problems of Atomic Science and Technology. Series "Plasma Physics" (13).* 2007, N 1, p. 151-153.

4. John B. Boffard, R.O. Jung, Chun C. Lin, A.E. Wendl. Optical emission measurements of electron energy distributions in low-pressure argon inductively coupled plasmas // *Plasma Sources Sci. Technol.* 2010, v. 19, p. 065001. DOI: 10.1088/0963-0252/19/6/065001



*Article received 15.10.2024*


## ПРОСТОРОВИЙ РОЗПОДІЛ ЕЛЕКТРИЧНОГО ПОЛЯ В ДВОСТУПЕНЕВОМУ ДЖЕРЕЛІ ПЛАЗМИ ХОЛЛІВСЬКОГО ТИПУ


***В.Ю. Баженов, А.М. Добровольський, В.В. Ціолко, В.М. Піун***



Експериментально досліджено двоступеневе джерело плазми холлівського типу, що має спільний анод і два катоди, розташовані в місцях із суттєво різною конфігурацією магнітного поля. Розглянуто особливості просторового розподілу плаваючого потенціалу, виміряного рухомими зондами Ленгмюра. Зокрема встановлено, що у середній площині анода на осі пристрою величина плаваючого потенціалу плазми складає до 95% анодної напруги.